

An Operational Classification and Quantification of Multipartite Entangled States

Gustavo Rigolin,^{*} Thiago R. de Oliveira,[†] and Marcos C. de Oliveira[‡]

*Departamento de Física da Matéria Condensada,
Instituto de Física Gleb Wataghin, Universidade Estadual de Campinas,
Caixa Postal: 6165, cep 13083-970, Campinas, São Paulo, Brazil*

The understanding of multipartite entanglement is still an open field of research. Both its characterization and quantification are not completely satisfactory yet. In this paper we shed new light on this problem by formalizing and extending an operational multipartite entanglement measure introduced in T. R. Oliveira, G. Rigolin, and M. C. Oliveira, Phys. Rev. A **73**, 010305(R) (2006), which is inspired by the global entanglement first presented in D. A. Meyer and N. R. Wallach, J. Math. Phys. **43**, 4273 (2002). Contrary to global entanglement, the main feature of this new measure lies in the fact that we study the mean linear entropy of *all* possible partitions of a multipartite system. This allows for the construction of an operational multipartite entanglement measure which, along with other properties, is able to distinguish among different multipartite entanglement states which global entanglement failed to discriminate and is maximum at the critical point of the Ising chain in a transverse magnetic field.

PACS numbers: 03.67.Mn, 03.65.Ud, 05.30.-d

I. INTRODUCTION

Since Schrödinger's seminal paper [1], entanglement was recognized to be at the heart of Quantum Mechanics (QM). For a long time, however, the study of entangled states was restricted to the conceptual foundations of QM [2, 3]. Only during the last two decades it became clear that entanglement can be seen as a resource which can be used to efficiently implement informational and computational tasks [4]. The understanding of the qualitative and quantitative aspects of entanglement, therefore, naturally became a fertile field of research.

Today, bipartite entangled states are quite well understood and good measures of entanglement for these systems are available, specially for qubits [5]. By bipartite states we refer to a quantum system partitioned in two subsystems A and B . If the partition is greater than two we have multipartite states.

The study of multipartite entangled states (MES), however, is not a simple extension of what was done for bipartite entangled states. One of the reasons for this difficulty lies in the fact that most of the tools available to study bipartite states are in general not useful for multipartite states (the Schmidt decomposition [6] is a good example). After considerable work we lack a deep comprehension of MES and new tools must be developed in order to capture the essential features of genuine multipartite entanglement (ME).

Even a qualitative characterization of MES is very complex since we do not have only one 'kind' of entanglement.

A first complication is the fact that we can have multi-

partite states where only a fraction of the subsystems are entangled. Consider a system which can be divided into N subsystems (an N -partite system). Let $|\Psi\rangle = |\phi_1\rangle \otimes \dots \otimes |\phi_p\rangle \otimes |\psi\rangle$ be a state in which $|\phi_i\rangle$, $1 \leq i \leq p$, is a state describing subsystem i and $|\psi\rangle$ is a state describing the other $N - p$ subsystems. If $|\psi\rangle$ is an entangled state than $|\Psi\rangle$ is called a p -separable state [7].

After discovering the value of p for a given multipartite state another complication shows up when we focus on $|\psi\rangle$ since its subsystems can be entangled in several inequivalent ways. For example, in the case of three qubits there are two paradigmatic MES which cannot be converted to each other via local operations and classical communication (LOCC)[8]. And if we go to four qubits, we have nine different types of entanglement, all of which cannot be converted to each other via LOCC [9].

Our aim in this paper is to shed new light on the characterization and quantification of MES. We intend to do this by formalizing and extending an *operational* ME measure introduced in Ref. [10]. We should emphasize that it is an operational measurement in the sense that it is easily computable, even for a multipartite state composed of many subsystems. This measure has several interesting features, two of which were already explored in Ref. [10]: it is maximum at the critical point of the Ising chain in a transverse magnetic field and, contrary to global entanglement [11], it can identify genuine MES. This new measure can be seen as an extension of global entanglement and we call it, from now on, generalized global entanglement: $E_G^{(n)}$. The reason for the previous notation will become clear in the next section.

Another important aspect of $E_G^{(n)}$ is the fact that it has an intuitive physical interpretation. We can relate it to the linear entropy of the pure state being studied as well as with the purities of the reduced n -qubit states obtained by tracing out the other subsystems [12, 13].

This paper is organized as follows. In Sec. II we define formally $E_G^{(n)}$ and extensively discuss many interesting

^{*}Electronic address: rigolin@ifi.unicamp.br

[†]Electronic address: tro@ifi.unicamp.br

[‡]Electronic address: marcos@ifi.unicamp.br

properties satisfied by the generalized global entanglement. In Sec. III we calculate $E_G^{(n)}$ for the most representatives MES. This gives us a good intuition of the meaning of $E_G^{(n)}$ and illustrates its usefulness. We also compare $E_G^{(n)}$ with other measures available, highlighting the main differences and the advantages and disadvantages of each one. Finally, in Sec. IV we present our final remarks and possible extensions and applications for $E_G^{(n)}$.

II. GENERALIZED GLOBAL ENTANGLEMENT

Global entanglement (GE) was introduced in Ref. [11] and then it was shown in Ref. [14] to be equivalent to the mean linear entropy (LE) of a single qubit of the chain. This connection between GE and LE considerably simplified the calculation of GE and also extended it to systems of higher dimensions because LE is not restricted only to qubits. An intuitive, though not so rigorous, way of understanding GE is to consider it as quantifying the mean entanglement between one subsystem with the rest of the subsystems. In this process we are dividing a system of N components into a single subsystem and the remaining $N - 1$. We can, nevertheless, separate the system into two blocks, one containing L subsystems and the other one $N - L$ [17, 18].

However, we have many different ways of constructing a given ‘block’. In Refs. [17, 18] a block of L subsystems consisted of the first L successive subsystems: $L = \{S_1, S_2, S_3, \dots, S_L\}$. But we can have any possible combination of L subsystem to construct a block. We may have, for instance, a ‘block’ formed by the first L odd subsystems: $L = \{S_1, S_3, S_5, \dots, S_{2L-1}\}$. It is legitimate to compute the LE of each one of these possible partitions. Roughly speaking this allows us to detect and quantify all possible ‘types’ of entanglement in a multipartite pure state.

In this section we introduce the generalized global entanglement ($E_G^{(n)}$), which is defined to take account of all those possible partitions of a system composed of N subsystems. We highlight two main important qualities of $E_G^{(n)}$: (a) It is a relatively simple and operational measure. Since it is based on LE it can be easily evaluated and is valid for any type of multipartite pure state (states

belonging either to finite or infinite dimension Hilbert spaces). (b) Each class of $E_G^{(n)}$ is related to the mixedness/purity of *all* possible n -partite reduced density matrices out of a system composed of N subsystems. It is not restricted to reduced density matrices of only one subsystem as the original GE [11, 12, 13]. This fact helps us in the physical understanding of $E_G^{(n)}$.

Following the definition of $E_G^{(n)}$ we move to the study of the general properties of this new measure relating it to the mixedness/purity of the various reduced density matrices of the system. After that we particularize to qubits focusing on the ability of the generalized global entanglement to classify and quantify MES. We end this section presenting a variety of examples which clarifies the necessity of all the classes of $E_G^{(n)}$, i. e. $n = 1, 2, 3, \dots$, to properly understand the many facets of MES.

A. Formal Definition of The Measure

Consider a system S which is partitioned in N subsystems S_i , $1 \leq i \leq N$. Let $|\Psi\rangle \in \mathcal{H}$ be a quantum state describing S and \mathcal{H} the Hilbert space of the whole system. Since we have N subsystems, $\mathcal{H} = \mathcal{H}_1 \otimes \dots \otimes \mathcal{H}_N = \bigotimes_{i=1}^N \mathcal{H}_i$, in which \mathcal{H}_i is the Hilbert space associated with S_i . The density matrix of S is $\rho = |\Psi\rangle\langle\Psi|$ and we define the generalized global entanglement as,

$$E_G^{(n)}(\rho) = \frac{1}{C_{n-1}^{N-1}} \sum_{i_1=1}^{N-1} \sum_{i_2=i_1+1}^{N-1} \sum_{i_3=i_2+1}^{N-1} \dots \dots \sum_{i_{n-1}=i_{n-2}+1}^{N-1} G(n, i_1, i_2, \dots, i_{n-1}). \quad (1)$$

Here all the parameters are natural numbers, $n < N$, and

$$C_{n-1}^{N-1} = \frac{(N-1)!}{(N-n)!(n-1)!}$$

is the definition of the binomial coefficient. Note that the summation is over all i_k 's, with the restriction that $1 \leq i_1 < i_2 < \dots < i_{n-1} \leq N - 1$. We also assume $i_0 = 0$.

The function G is given as,

$$G(n, i_1, i_2, \dots, i_{n-1}) = \frac{d}{d-1} \left[1 - \frac{1}{N - i_{n-1}} \sum_{j=1}^{N-i_{n-1}} \text{Tr} \left(\rho_{j, j+i_1, j+i_2, \dots, j+i_{n-1}}^2 \right) \right], \quad (2)$$

where $\rho_{j, j+i_1, j+i_2, \dots, j+i_{n-1}}$ is obtained tracing out all the subsystems but $S_A = \{S_j, S_{j+i_1}, S_{j+i_2}, \dots, S_{j+i_{n-1}}\}$ and

$d = \min\{\dim S_A, \dim \bar{S}_A\}$. Here $\dim S_A$ and $\dim \bar{S}_A$ are, respectively, the Hilbert space dimension of the subsys-

tem S_A and of its complement \overline{S}_A .

B. General Properties

Eqs. (1) and (2) are valid for any multipartite pure system, even systems described by continuous variables (Gaussian states for example). The key concept behind generalized global entanglement is the fact that it is based on linear entropy (LE), which is an entanglement monotone easily calculated for the vast majority of pure states. Thus, by its very definition, $E_G^{(n)}$ and G inherit all the properties satisfied by LE, including the crux of all entanglement monotones: non-increase under LOCC.

Another important concept of E_G^n and G is the introduction of classes of multipartite entanglement (ME) labeled by the index n . As we will see, they are related with the many ways a multipartite state can be entangled. Moreover, a genuine multipartite entangled state (MES) must have non-zero $E_G^{(n)}$ and G 's for all classes n .

Before we proceed, we should mention what we understand by a genuine MES. It is a pure entangled system in which no pure state can be defined to anyone of its subsystems. There is only one pure state describing the whole system. For three qubits, for instance, the states $|GHZ\rangle = (1/\sqrt{2})(|000\rangle + |111\rangle)$ and $|W\rangle = (1/\sqrt{3})(|001\rangle + |010\rangle + |100\rangle)$ are genuine MES but $|\xi\rangle = (1/\sqrt{2})(|00\rangle + |11\rangle)|0\rangle$ is not.

Let us now explicitly show how the first classes of $E_G^{(n)}$ look like. This will clarify the physical meaning of the measure as well as the intuitive aspects which led us to arrive at the general and formal definitions given in Eqs. (1) and (2).

1. First Class: $n = 1$

When $n = 1$ Eqs. (1) and (2) are the same,

$$E_G^{(1)}(\rho) = G(1) = \frac{d}{d-1} \left[1 - \frac{1}{N} \sum_{j=1}^N \text{Tr}(\rho_j^2) \right], \quad (3)$$

and if we remember the definition of the linear entropy of the subsystem j with the rest of the other subsystems [14, 15],

$$E_L(\rho_j) = \frac{d}{d-1} [1 - \text{Tr}(\rho_j^2)], \quad (4)$$

Eq. (3) can be written as [10]

$$E_G^{(1)} = \frac{1}{N} \sum_{j=1}^N E_L(\rho_j) = \langle E_L(\rho_j) \rangle. \quad (5)$$

In other words, $E_G^{(1)}$ is simply the mean linear entropies of all the subsystems S_j . We should mention that for

qubits ($d = 2$), $E_G^{(1)}$ was shown to be [14] exactly the Meyer and Wallach global entanglement [11].

The physical intuition behind the study of the mean linear entropies lies in the fact that the more a state is a genuine MES the more mixed their reduced density matrices should be. However, we should not limit ourselves to evaluating the reduced density matrices of single subsystems S_j . We can take two, three, n subsystems and calculate their reduced density matrices and also calculate their mean linear entropies. This is the reason of why we introduce the other classes of generalized global entanglement. And we insist, a genuine MES should have non-zero entanglement for all classes.

2. Second Class: $n = 2$

For $n = 2$ Eqs. (1) and (2) are not identical anymore, being, nevertheless, entanglement monotones:

$$E_G^{(2)}(\rho) = \frac{1}{N-1} \sum_{i_1=1}^{N-1} G(2, i_1), \quad (6)$$

$$G(2, i_1) = \frac{d}{d-1} \left[1 - \frac{1}{N-i_1} \sum_{j=1}^{N-i_1} \text{Tr}(\rho_{j,j+i_1}^2) \right]. \quad (7)$$

Now we deal with reduced density matrices of the subsystems S_j and S_{j+i_1} . The extra parameter i_1 is introduced to take account of the many possible 'distances' between the two subsystems. For nearest neighbors $i_1 = 1$, next-nearest neighbors $i_2 = 2$, and so forth.

Noting that the linear entropy of the subsystems S_j and S_{j+i_1} with the rest of the other subsystem is given by

$$E_L(\rho_{j,j+i_1}) = \frac{d}{d-1} [1 - \text{Tr}(\rho_{j,j+i_1}^2)], \quad (8)$$

Eq. (7) can be written as,

$$G(2, i_1) = \frac{1}{N-i_1} \sum_{j=1}^{N-i_1} E_L(\rho_{j,j+i_1}) = \langle E_L(\rho_{j,j+i_1}) \rangle. \quad (9)$$

This implies that Eq. (6) is simply,

$$E_G^{(2)}(\rho) = \frac{1}{N-1} \sum_{i_1=1}^{N-1} \langle E_L(\rho_{j,j+i_1}) \rangle = \langle \langle E_L(\rho_{j,j+i_1}) \rangle \rangle. \quad (10)$$

Looking at Eqs. (9) and (10) we can easily interpret $E_G^{(2)}$ and $G(2, i_1)$. First, let us deal with $G(2, i_1)$. We assume all the subsystems are organized in a linear chain. (This assumption simplifies the discussion in what follows and can be relaxed.) If we remember that $1 \leq i_1 \leq N-1$, where N is the number of subsystems, Eq. (9) tells us

that $G(2, i_1)$ is nothing but the mean linear entropy of two subsystems with the rest of the other subsystems conditioned on that these two subsystems are i_1 lattice sites apart.

For concreteness, let us explicitly write all the possible $G(2, i_1)$ for a linear chain of five subsystems. Since $N = 5$ we have $1 \leq i_1 \leq 4$, giving us four G 's:

- (1) $G(2, 1)$, which is the mean linear entropy (LE) of the following pairs of subsystems with the rest of the chain: $\{(S_1, S_2), (S_2, S_3), (S_3, S_4), (S_4, S_5)\}$;
- (2) $G(2, 2)$, which is the mean LE of the following pairs of subsystems: $\{(S_1, S_3), (S_2, S_4), (S_3, S_5)\}$;
- (3) $G(2, 3)$, which is the mean LE of the following pairs of subsystems: $\{(S_1, S_4), (S_2, S_5)\}$;
- (4) $G(2, 4)$, which is the mean LE of the following pairs of subsystems: $\{(S_1, S_5)\}$.

See Fig. 1 for a pictorial representation of all possible combinations of two subsystems out of five.

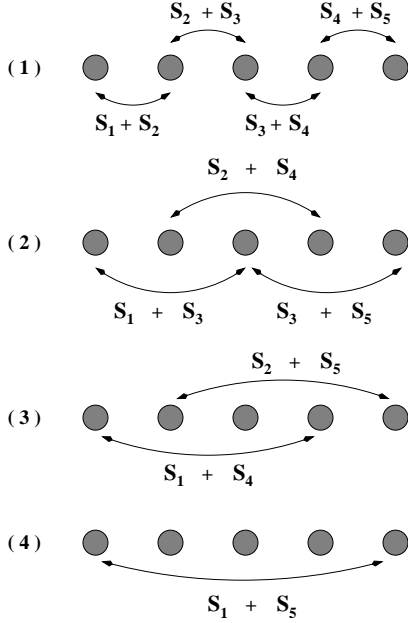


Figure 1: All combinations of two elements out of five.

Finally, Eq. (10) shows that $E_G^{(2)}$ is the mean linear entropy of two subsystems with the rest of the chain irrespective of the distance between the two subsystems.

3. Third Class: $n = 3$

Setting $n = 3$ Eqs. (1) and (2) become,

$$E_G^{(3)}(\rho) = \frac{2}{(N-1)(N-2)} \sum_{i_1=1}^{N-1} \sum_{i_2=i_1+1}^{N-1} G(n, i_1, i_2), \quad (11)$$

$$G(3, i_1, i_2) = \frac{d}{d-1} \left[1 - \frac{1}{N-i_2} \sum_{j=1}^{N-i_2} \text{Tr}(\rho_{j, j+i_1, j+i_2}^2) \right]. \quad (12)$$

Looking at Eq. (12) we see that we are now dealing with reduced density matrices of three subsystems: S_j , S_{j+i_1} , and S_{j+i_2} . Therefore, $G(3, i_1, i_2)$ is the mean linear entropy of all three subsystems with the rest of the chain conditioned that S_{j+i_1} and S_{j+i_2} are, respectively, i_1 and i_2 lattice sites apart from S_j . Taking the mean of all possible $G(3, i_1, i_2)$ we get Eq. (11). This is equivalent to averaging over all linear entropies of three subsystems irrespective of their distances. Although we do not write them here, similar expressions as those given by Eqs. (9) and (10) can be obtained for this class.

Again, as we did for the second class, it is explanatory to analyze in details the $N = 5$ case. Now $1 \leq i_1 < i_2 \leq 4$. This time we have six G 's (See Fig. 2):

- (1) $G(3, 1, 2)$, which is the mean linear entropy (LE) of the following triples of subsystems with the rest of the chain: $\{(S_1, S_2, S_3), (S_2, S_3, S_4), (S_3, S_4, S_5)\}$;
- (2) $G(3, 1, 3)$, which is the mean LE of the following triples of subsystems: $\{(S_1, S_2, S_4), (S_2, S_3, S_5)\}$;
- (3) $G(3, 1, 4)$, which is the mean LE of the following triples of subsystems: $\{(S_1, S_2, S_5)\}$;
- (4) $G(3, 2, 3)$, which is the mean LE of the following triples of subsystems: $\{(S_1, S_3, S_4), (S_2, S_4, S_5)\}$;
- (5) $G(3, 2, 4)$, which is the mean LE of the following triples of subsystems: $\{(S_1, S_3, S_5)\}$;
- (6) $G(3, 3, 4)$, which is the mean LE of the following triples of subsystems: $\{(S_1, S_4, S_5)\}$.

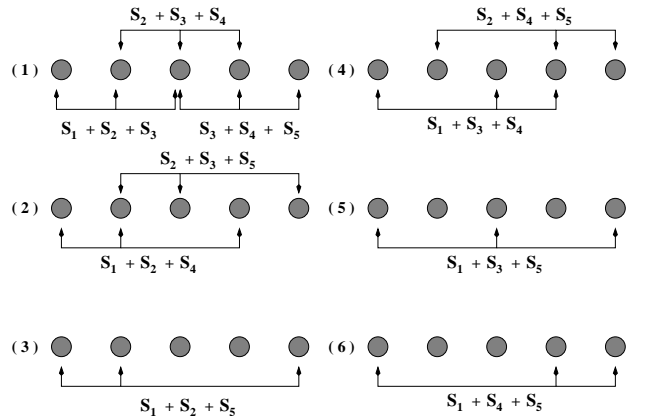


Figure 2: All combinations of three elements out of five.

4. Higher Classes: $n \geq 4$

Remembering that $n < N$, higher classes just make sense for systems composed of more and more subsystems. And the higher a class the greater the number of G 's we will find. This is a satisfactory property we should expect from a useful entanglement measure since as we increase the number of partitions of a system we increase the way it may be entangled [8, 9].

If we employ the definition of LE for n subsystems out of a total of N ,

$$E_L(\rho_{j,\dots,j+i_{n-1}}) = \frac{d}{d-1} \left[1 - \text{Tr} \left(\rho_{j,\dots,j+i_{n-1}}^2 \right) \right], \quad (13)$$

we can write Eqs. (2) and (1) as,

$$G(n, i_1, \dots, i_{n-1}) = \langle E_L(\rho_{j,j+i_1,\dots,i_{n-1}}) \rangle, \quad (14)$$

$$E_G^{(n)}(\rho) = \langle \langle E_L(\rho_{j,j+i_1,\dots,i_{n-1}}) \rangle \rangle. \quad (15)$$

In Eq. (14) the single pair of brackets $\langle \rangle$ represents the averaging over all possible configurations of n subsystems in which subsystem S_{j+i_k} is i_k lattice sites apart from S_j . Here $1 < k < n-1$. Finally, the double brackets $\langle \langle \rangle \rangle$ is the average of the linear entropy of n subsystems over all possible combinations (distances) in which they can be arranged.

We should mention at this point that $E_G^{(n)}$ and G are more general than the block entanglement ($E_B^{(n)}$) as presented in Refs. [16, 17, 18]. By block entanglement it is understood that we divide a set of N subsystems $\{S_1, S_2, \dots, S_N\}$ in two blocks, $A_n = \{S_1, S_2, \dots, S_n\}$ and $B_{N-n} = \{S_{n+1}, S_{n+2}, \dots, S_N\}$, and calculate the linear or von Neumann entropy between blocks A_n and B_{N-n} . In the language of generalized global entanglement, block entanglement for a translational symmetric state is simply

$$E_B^{(n)} = G(n, i_1 = 1, i_2 = 1, \dots, i_{n-1} = 1),$$

which is only one of the many G 's we can define. The main difference between these two measures lies in the fact that we allow all possible combinations of n subsystems out of N to represent a possible 'block'. Contrary to block entanglement, here there exists no restriction onto the subsystems belonging to a given 'block' to be nearest neighbors.

C. Particular Properties for Qubits

Although Eqs. (1) and (2) are valid for qudits and continuous variable systems, we now focus on some properties of $E_G^{(n)}$ and G assuming that we deal with qubits. There are two main reasons for studying qubits in detail. First, they are recognized as a key concept on quantum information theory and second, the simplest multipartite states are constructed employing qubits.

Let $\rho = |\Psi\rangle\langle\Psi|$ be the density matrix of a N qubit system and $\rho_j = \text{Tr}_{\bar{j}}(\rho)$ the reduced density matrix of subsystem S_j , which is obtained tracing out all subsystems but S_j .

A general one qubit density matrix can be written as,

$$\rho_j = \text{Tr}_{\bar{j}}(\rho) = \frac{1}{2} \sum_{\alpha} p_j^{\alpha} \sigma_j^{\alpha}, \quad (16)$$

where the coefficients are given by

$$p_j^{\alpha} = \text{Tr}(\sigma_j^{\alpha} \rho_j) = \langle \Psi | \sigma_j^{\alpha} | \Psi \rangle. \quad (17)$$

Here σ_j^{α} is the Pauli matrix acting on the site j , $\alpha = 0, x, y, z$, where σ^0 is the identity matrix of dimension two, and p_{α} is real. Since ρ_j is normalized $p_0 = 1$. Using Eqs. (16) and (17) we obtain

$$\text{Tr}(\rho_j^2) = \frac{1}{2} (1 + \langle \sigma_j^x \rangle^2 + \langle \sigma_j^y \rangle^2 + \langle \sigma_j^z \rangle^2). \quad (18)$$

This last result implies that Eq. (3) can be written as

$$E_G^{(1)} = 1 - \frac{1}{N} \sum_{j=1}^N (\langle \sigma_j^x \rangle^2 + \langle \sigma_j^y \rangle^2 + \langle \sigma_j^z \rangle^2). \quad (19)$$

One interesting situation occurs when we have translational invariant states ρ . (The Ising model ground state for example.) In this scenario $\langle \sigma_i^{\alpha} \rangle = \langle \sigma_j^{\alpha} \rangle$ for any i and j . Therefore, Eq. (19) becomes

$$E_G^{(1)} = 1 - \langle \sigma_j^x \rangle^2 - \langle \sigma_j^y \rangle^2 - \langle \sigma_j^z \rangle^2, \quad (20)$$

which is related to the total magnetization M of the system: $|M|^2 = N(\langle \sigma_j^x \rangle^2 + \langle \sigma_j^y \rangle^2 + \langle \sigma_j^z \rangle^2)$.

Tracing out all subsystems but S_i and S_j we obtain the two qubit reduced density matrix

$$\rho_{ij} = \text{Tr}_{\bar{ij}}(\rho) = \frac{1}{4} \sum_{\alpha, \beta} p_{ij}^{\alpha\beta} \sigma_i^{\alpha} \otimes \sigma_j^{\beta}, \quad (21)$$

where

$$p_{ij}^{\alpha\beta} = \text{Tr}(\sigma_i^{\alpha} \sigma_j^{\beta} \rho_{ij}) = \langle \Psi | \sigma_i^{\alpha} \sigma_j^{\beta} | \Psi \rangle. \quad (22)$$

Eq. (21) is the most general way to represent a two-qubit state and together with Eq. (22) imply that

$$\text{Tr}(\rho_{ij}^2) = \frac{1}{4} \sum_{\alpha, \beta} \langle \sigma_i^{\alpha} \sigma_j^{\beta} \rangle^2. \quad (23)$$

If we pay attention to Eq. (23) we will note that the trace of ρ_{ij}^2 is the sum of all one and two-point correlation functions. Moreover, since $E_G^{(2)}$ and $G(2, i_1)$ depends on Eq. (23), we find in these entanglement measures both diagonal and off-diagonal correlation functions.

Again it is instructive to study translational symmetric states in which $p_{ij}^{\alpha\beta} = p_{ij}^{\beta\alpha}$ for any α and β (The Ising

model is a paradigmatic example). Using this assumption in Eq. (7) we get

$$G(2, i_1) = 1 - \frac{2}{3} [\langle \sigma_j^x \rangle^2 + \langle \sigma_j^y \rangle^2 + \langle \sigma_j^z \rangle^2 + \langle \sigma_j^x \sigma_{j+i_1}^y \rangle^2 + \langle \sigma_j^x \sigma_{j+i_1}^z \rangle^2 + \langle \sigma_j^y \sigma_{j+i_1}^z \rangle^2 + \langle \sigma_j^x \sigma_{j+i_1}^x \rangle^2 / 2 + \langle \sigma_j^y \sigma_{j+i_1}^y \rangle^2 / 2 + \langle \sigma_j^z \sigma_{j+i_1}^z \rangle^2 / 2]. \quad (24)$$

Note that the previous formula is not valid for $N \leq 3$. For $N = 2$ only $E_G^{(1)}$ is defined and for $N = 3$ we have $d = \min\{\dim S_A, \dim \bar{S}_A\} = 2$ and not $d = 4$, the value of d for all $N \geq 4$.

If we compare $G(2, i_1)$ with the concurrence (a bipartite entanglement monotone) for the Ising model we will note that it does not depend on any off-diagonal two-point correlation function [19, 20]. This fact highlights the importance of the off-diagonal correlations in the quantification of ME.

D. Why Do We Need Higher Classes?

The simple fact that different types of entanglement appear as we increase the number of qubits (or equivalently the number of subsystems) [8, 9] indicates that the various classes here introduced may be useful to classify and quantify the many facets of ME.

The first class, for example, does not suffice to unequivocally quantify MES. Although $E_G^{(1)}$ is maximal for Greenberger-Horne-Zeilinger (GHZ) states [21] it is also maximal for a state which is not a MES.

In order to better understand this point let us study $E_G^{(1)}$ for three paradigmatic multipartite states. The first one is the GHZ state:

$$|GHZ_N\rangle = \frac{1}{\sqrt{2}} (|0\rangle^{\otimes N} + |1\rangle^{\otimes N}), \quad (25)$$

where $|0\rangle^{\otimes N}$ and $|1\rangle^{\otimes N}$ represent, respectively, N tensor products of the states $|0\rangle$ and $|1\rangle$. The GHZ state is a genuine MES since by measuring only one of the qubits in the standard basis we know exactly the results of the other $N - 1$ qubits. Furthermore, tracing out any one of the qubits we obtain a separable state. A direct calculation gives $E_G^{(1)}(GHZ_N) = 1$.

The second state we shall analyze is given by a tensor product of $N/2$ Einstein-Podolsky-Rosen (EPR) Bell states [12]:

$$|EPR_N\rangle = |\Phi^+\rangle \otimes \dots \otimes |\Phi^+\rangle = |\Phi^+\rangle^{\otimes \frac{N}{2}}, \quad (26)$$

where $|\phi^+\rangle = (1/\sqrt{2})(|00\rangle + |11\rangle)$. For definiteness, we chose one specific Bell state. However, the results here derived are quite general and valid for any $N/2$ tensor products of Bell states. This state obviously is not a MES. Only the pairs of qubits $(2j - 1, 2j)$, where $j = 1, 2, \dots, N/2$, are entangled. Nevertheless, we again obtain $E_G^{(1)}(EPR_N) = 1$. This last result illustrates that the

maximality of $E_G^{(1)}$ is not a sufficient condition to detect genuine MES. Note that $E_G^{(1)}$ for both the GHZ_N and EPR_N states are independent of the number of qubits N in the chain.

The last state we consider is the W state [8]. It is defined as,

$$|W_N\rangle = \frac{1}{\sqrt{N}} \sum_{j=1}^N |000 \dots 1_j \dots 000\rangle. \quad (27)$$

The state $|000 \dots 1_j \dots 000\rangle$ represents a N qubit state in which the j -th qubit is $|1\rangle$ and all the others are $|0\rangle$. As shown in Ref. [11], $E_G^{(1)}(W_N) = 4(N - 1)/N^2$. Note that $E_G^{(1)}$ depends on N and at the thermodynamic limit ($N \rightarrow \infty$) we have $E_G^{(1)}(W_N) = 0$. For three qubits, the W state was shown [8] to be a genuine MES not convertible via LOCC to a GHZ state.

Calculating $E_G^{(2)}$ and $G(2, 1)$ for the previous states above we see that now we have different values of $E_G^{(2)}$ and $G(2, 1)$ for each one of them. Note that for $N = 2$ the previous functions are not defined and that for $N = 3$ $E_G^{(2)} = G(2, 1) = 1$. Table I shows $E_G^{(2)}$ and $G(2, 1)$ for the states GHZ_N , EPR_N , and W_N . We should mention that due to translational symmetry, $G(2, 1)$ and $E_G^{(2)}$ are identical for the states GHZ_N and W_N .

Table I: The third and fourth columns give $G(2, 1)$ and $E_G^{(2)}$ for the three states listed in the first column when $N > 3$. The second column gives $E_G^{(1)}$ for all N . Contrary to $E_G^{(1)}$, we see that $G(2, 1)$ and $E_G^{(2)}$ distinguish the three states from each other.

	$E_G^{(1)}$	$G(2, 1)$	$E_G^{(2)}$
GHZ_N	1	$\frac{2}{3}$	$\frac{2}{3}$
EPR_N	1	$\frac{N-2}{2(N-1)}$	$\frac{(2N-1)(N-2)}{2(N-1)^2}$
W_N	$\frac{4(N-1)}{N^2}$	$\frac{16(N-2)}{3N^2}$	$\frac{16(N-2)}{3N^2}$

It is interesting to note that depending on the value of N , the states are differently classified. Fig. 3 illustrates this point. A similar behavior is observed for $E_G^{(2)}$ (Fig. 4). In this case, however, EPR_N is the most entangled state for long chains. The reason for this lies in the definition of $E_G^{(2)}$. For the EPR_N state, $G(2, l) = 1$ for any $l \geq 2$. Therefore, since $E_G^{(2)}$ is obtained averaging over all $G(2, l)$, for long chains $G(2, 1)$ does not contribute much and $E_G^{(2)} \rightarrow 1$.

We also calculated the values of $E_G^{(1)}$, $E_G^{(2)}$, and $G(2, 1)$ at the thermodynamic limit. See Tab. II.

It is worth mentioning that even at the thermodynamic limit $E_G^{(2)}$ and $G(2, 1)$ distinguish the three states. The ordering of the states, nevertheless, is different. Again

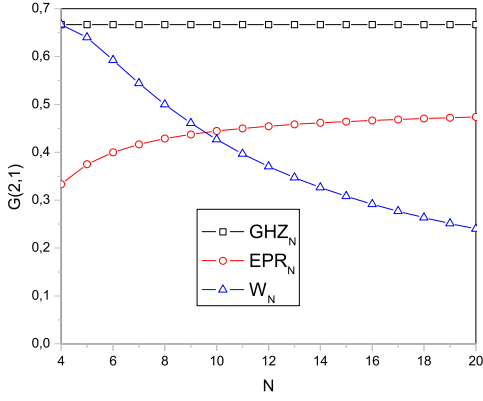


Figure 3: (Color online) Here we show $G(2,1)$ as a function of the number of qubits N for the states GHZ_N , EPR_N and W_N . Note that only when $N = 4$ we have two states with the same entanglement. Furthermore, for $4 \leq N \leq 8$, W_N is more entangled than EPR_N . This ordering is changed for $N \geq 9$.

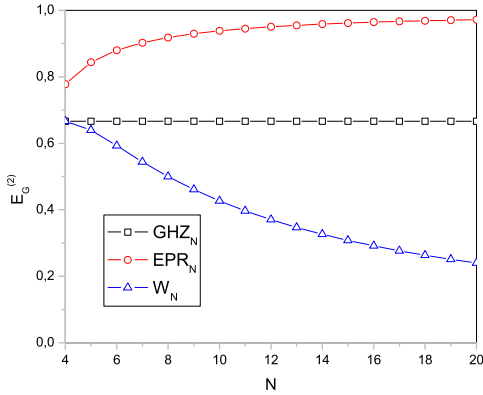


Figure 4: (Color online) Here we show $E_G^{(2)}$ as a function of N . Again, only when $N = 4$ we have two states with the same entanglement. Moreover, for $N \geq 4$, EPR_N is the most entangled state.

Table II: $E_G^{(1)}$, $G(2,1)$, and $E_G^{(2)}$ at the thermodynamic limit.

$N \rightarrow \infty$	$E_G^{(1)}$	$G(2,1)$	$E_G^{(2)}$
GHZ_N	1	2/3	2/3
EPR_N	1	1/2	1
W_N	0	0	0

this is related to the definition of $E_G^{(2)}$ and is due to the contribution of $G(2,l)$, $l \geq 2$, in the calculation of $E_G^{(2)}(EPR_N)$.

Let us now consider the following two states,

$$\begin{aligned}
 |EPR_2\rangle &= |\Phi^+\rangle_{12}|\Phi^+\rangle_{34} \\
 &= \frac{1}{2}(|0\rangle_1|0\rangle_2|0\rangle_3|0\rangle_4 + |0\rangle_1|0\rangle_2|1\rangle_3|1\rangle_4 \\
 &\quad + |1\rangle_1|1\rangle_2|0\rangle_3|0\rangle_4 + |1\rangle_1|1\rangle_2|1\rangle_3|1\rangle_4), \quad (28)
 \end{aligned}$$

which is a pair of EPR states where subsystem S_1 is

entangled with S_2 and S_3 is entangled with S_4 . The other state is [22],

$$\begin{aligned}
 |g_1\rangle &= \frac{1}{2}(|0\rangle_1|0\rangle_2|0\rangle_3|0\rangle_4 + |0\rangle_1|1\rangle_2|0\rangle_3|1\rangle_4 \\
 &\quad + |1\rangle_1|0\rangle_2|1\rangle_3|0\rangle_4 + |1\rangle_1|1\rangle_2|1\rangle_3|1\rangle_4) \\
 &= \frac{1}{2}(|0\rangle_1|0\rangle_3|0\rangle_2|0\rangle_4 + |0\rangle_1|0\rangle_3|1\rangle_2|1\rangle_4 \\
 &\quad + |1\rangle_1|1\rangle_3|0\rangle_2|0\rangle_4 + |1\rangle_1|1\rangle_3|1\rangle_2|1\rangle_4) \\
 &= |\Phi^+\rangle_{13}|\Phi^+\rangle_{24}. \quad (29)
 \end{aligned}$$

Again we have two EPR states. But now, however, subsystem S_1 is entangled with S_3 and subsystem S_2 is entangled with S_4 (See Fig. 5).

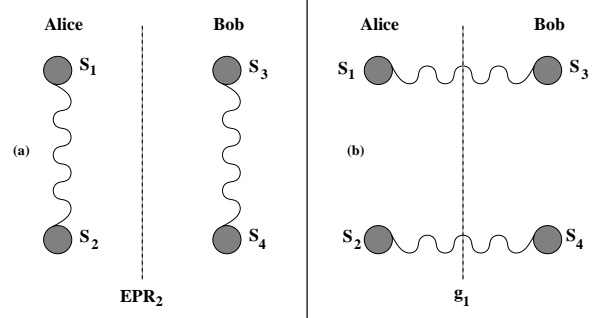


Figure 5: Pictorial representations of the states (a) EPR_2 and (b) g_1 .

Although different pairs of subsystems are entangled in the previous two states, their amount of entanglement is the same: we have two EPR states in both cases. This fact is captured by the entanglement measures here introduced: $E_G^{(n)}(EPR_2) = E_G^{(n)}(g_1)$. The block entanglement, nevertheless, does not always give the same value for the two states above (Tab. III). This example illus-

Table III: Comparison between $E_G^{(n)}$, $G(2,1)$, and $E_B^{(n)}$

	$E_G^{(1)}$	$E_G^{(2)}$	$G(2,1)$	$E_B^{(1)}$	$E_B^{(2)}$
EPR_2	1	7/9	1/3	1	0
g_1	1	7/9	1/3	1	1

trates that the block entanglement, as its name suggests, quantifies only the entanglement of partition A (sites 1 and 2) with partition B (sites 3 and 4). The generalized global entanglement $E_G^{(n)}$ quantifies, however, the entanglement of a state independent of the way it is distributed among the subsystems.

We can go further and show the importance of using higher classes to correctly quantify the entanglement of a multipartite state no matter how the entanglement is distributed among the subsystems. For example, consider the state

$$|GHZ_N^M\rangle = |GHZ_N\rangle^{\otimes M}, \quad (30)$$

where the integer $M \geq 1$ represents how many tensor products of GHZ_N we have. Restricting ourselves to $N = 3$ and $M = 2$ we get,

$$\begin{aligned} |GHZ_3^2\rangle &= \frac{1}{\sqrt{2}}(|000\rangle + |111\rangle) \otimes \frac{1}{\sqrt{2}}(|000\rangle + |111\rangle) \\ &= \frac{1}{2}(|000000\rangle + |000111\rangle + |111000\rangle \\ &\quad + |111111\rangle). \end{aligned} \quad (31)$$

Here, subsystems $S_1, S_2,$ and S_3 form a genuine MES and $S_4, S_5,$ and S_6 another one. For this state $E_B^{(3)} = 0$. If we interchange the second qubit with the fifth one we will obtain the following state:

$$\begin{aligned} |ZHG_3^2\rangle &= \frac{1}{2}(|000000\rangle + |010101\rangle + |101010\rangle \\ &\quad + |111111\rangle). \end{aligned} \quad (32)$$

Now subsystems $S_1, S_3,$ and S_5 form a genuine MES and $S_2, S_4,$ and S_6 another one (See Fig. 6).

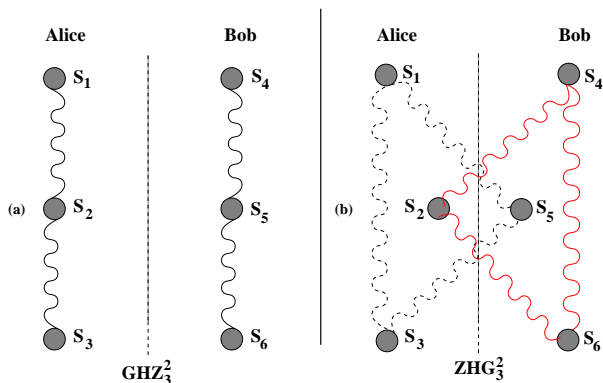


Figure 6: (Color online) Pictorial representations of the states (a) GHZ_3^2 and (b) ZHG_3^2 .

We still have the same amount of entanglement, i. e. two GHZ states. Calculating the block entanglement we get $E_B^{(3)} = 6/7$. Note that we have different $E_B^{(3)}$ for the previous two states. If we had employed the generalized global entanglement we would have obtained $E_G^{(3)}(GHZ_3^2) = E_G^{(3)}(ZHG_3^2)$. In general we have $E_B^{(n)}(GHZ_n^2) \neq E_B^{(n)}(ZHG_n^2)$ and $E_G^{(n)}(GHZ_n^2) = E_G^{(n)}(ZHG_n^2)$. Therefore, if we want to study the amount of entanglement of a multipartite state, independent of how it is distributed among the subsystems, we should employ $E_G^{(n)}$ and not $E_B^{(n)}$, since the last one furnishes only the amount of entanglement between the two blocks in which the system can be divided.

III. USEFULNESS OF GENERALIZED GLOBAL ENTANGLEMENT

In this section we present two examples in which we explore the utility of $E_G^{(n)}$ and the auxiliary measure

$G(n, i_1, i_2, \dots, i_{n-1})$. The first example deals with a finite chain of four qubits. We show that $E_G^{(2)}$ together with $G(2, 1)$ allow us to correctly identify MES. Moreover, comparing the values of $G(2, i_1)$ for all the MES here presented we are led to a practical definition of what is a genuine MES.

The second example is a study of the entanglement properties of the Ising model ground state. We show that $E_G^{(2)}$ and $G(2, i_1)$ are maximal at the critical point and we analyze what correlation functions are responsible for this behavior of the generalized global entanglement. The results herein presented suggests that the long range correlations in the critical point for the Ising model are related to genuine MES.

A. Finite Chains

Let us now focus on the simplest non-trivial spin-1/2 chain, i. e. states with $N = 4$ qubits, by studying the entanglement properties of four genuine MES [23, 24].

The first one [23] is the famous four qubit GHZ state [21],

$$|GHZ_4\rangle = |\Phi_1\rangle = \frac{1}{\sqrt{2}}(|0000\rangle + |1111\rangle). \quad (33)$$

The qualitative and quantitative features of this state were discussed in Sec. IID. A direct calculation gives $E_G^{(1)}(\Phi_1) = 1; E_G^{(2)}(\Phi_1) = G(2, i_1)(\Phi_1) = 2/3$, where $i_1 = 1, 2, 3$.

The second state [23] is written as,

$$\begin{aligned} |\Phi_2\rangle &= \frac{1}{\sqrt{6}}\left(\sqrt{2}|1111\rangle + |1000\rangle + |0100\rangle + |0010\rangle \right. \\ &\quad \left. + |0001\rangle\right). \end{aligned} \quad (34)$$

Calculating its first and second order generalized global entanglement we obtain $E_G^{(1)}(\Phi_2) = 1; E_G^{(2)}(\Phi_2) = G(2, i_1)(\Phi_2) = 8/9$. Note that as well as $|\Phi_1\rangle$ this state is a translational symmetric state. Moreover, $G(2, i_1)(\Phi_2) \geq G(2, i_1)(\Phi_1)$. This last result will turn out to be very useful in constructing an operational definition of MES.

The third state [23] is given as,

$$|\Phi_3\rangle = \frac{1}{2}(|1111\rangle + |1100\rangle + |0010\rangle + |0001\rangle). \quad (35)$$

Since now we do not have a translational symmetric state $G(2, i_1)$ are not all equal. After a straightforward calculation we get $E_G^{(1)}(\Phi_3) = 1; E_G^{(2)}(\Phi_3) = 25/27; G(2, 1)(\Phi_3) = 7/9; G(2, 2)(\Phi_3) = G(2, 3)(\Phi_3) = 1$. Again we should note that $G(2, i_1)(\Phi_3) \geq G(2, i_1)(\Phi_1)$.

These three states have some remarkable properties [23]: (a) The local density operator describing each qubit are the maximally mixed state $(1/2)I_2$, where I_2 is the 2×2 identity matrix. That is why we have for all of them

$E_G^{(1)} = 1$. (b) The other reduced operators (with two and three qubits) do not have any k -tangle [25], $k = 2, 3$. This emphasizes that we really have genuine MES, i. e. there is no pairwise or triplewise entanglement. (c) They cannot be transformed into one another by LOCC.

The fourth and last state we shall consider,

$$|\chi\rangle = \frac{1}{2\sqrt{2}} (|0000\rangle - |0011\rangle - |0101\rangle + |0110\rangle + |1001\rangle + |1010\rangle + |1100\rangle + |1111\rangle), \quad (36)$$

was recently introduced and extensively studied by Ref. [24]. The main feature of this state lies in its usefulness to teleport an arbitrary two-qubit state. Employing χ this task can be accomplished either from subsystems S_1 and S_2 to S_3 and S_4 or from S_1 and S_3 to S_2 and S_4 . The usual channel (two Bell states) used to teleport an arbitrary two-qubit state [22, 26] can teleport two qubits only from a specific location to another one: from S_1 and S_2 to S_3 and S_4 for example.

In addition to this the previous state has a hybrid behavior in the sense that it resembles both the GHZ and W states [24]. Tracing out any one of the qubits the remaining reduced density matrix σ has maximal entropy, a characteristic of the GHZ state. However, σ has a non-zero negativity [27] between one qubit and the other two [24], a property of the W state.

Calculating the generalized global entanglement we obtain $E_G^{(1)}(\chi) = 1$; $E_G^{(2)}(\chi) = 23/27$; $G(2, 1)(\chi) = 8/9$; $G(2, 2)(\chi) = 1$; $G(2, 3)(\chi) = 2/3$. Again we see that for all i_1 we have $G(2, i_1)(\chi) \geq G(2, i_1)(\Phi_1)$.

We have grouped in Tab. IV the entanglement calculated for the previous four states.

Table IV: Calculated values of $E_G^{(n)}$ and $G(2, i_1)$ for the genuine MES shown in Sec. III A and for the EPR_2 state.

	$E_G^{(1)}$	$E_G^{(2)}$	$G(2, 1)$	$G(2, 2)$	$G(2, 3)$
EPR_2	1	$7/9 \approx 0.778$	$1/3$	1	1
Φ_1	1	$2/3 \approx 0.667$	$2/3$	$2/3$	$2/3$
Φ_2	1	$8/9 \approx 0.889$	$8/9$	$8/9$	$8/9$
Φ_3	1	$25/27 \approx 0.926$	$7/9$	1	1
χ	1	$23/27 \approx 0.852$	$8/9$	1	$2/3$

At this point we shall analyze carefully the information contained in Tab. IV. First of all, it should be clear that $E_G^{(1)}$ is not the last word concerning the quantification and classification of MES. A glimpse of the first column in Tab. IV shows that all the five states listed have $E_G^{(1)} = 1$, even the EPR_2 state, an obvious non-genuine MES. Therefore, since $E_G^{(1)} = 1$ is not useful to classify different genuine MES or to correctly identify them we are compelled to go further and study the higher classes of the generalized global entanglement in order to achieve such a goal.

Turning our attention to $E_G^{(2)}$ we see that it is different for all the five states listed in Tab. IV, implying that $E_G^{(2)}$

can distinguish among the five states. According to $E_G^{(2)}$ the most entangled state is Φ_3 , which was shown to be a genuine MES [23].

Moreover, important clues for the understanding of what kind of entanglement is present in a given multipartite state are also available in $G(2, i_1)$, $i_1 = 1, 2, 3$. Actually, these entanglement measures give us a more detailed view of the types of entanglement a state has than $E_G^{(2)}$ since the latter is an average over all $G(2, i_1)$.

For example, if we relied only on $E_G^{(2)}$ to decide whether or not a state is a genuine MES we would arrive at a wrong answer. This point is clearly demonstrated if we compare $E_G^{(2)}$ for the states EPR_2 and Φ_1 (GHZ_4). Looking at Tab. IV we see that $E_G^{(2)}(EPR_2) > E_G^{(2)}(\Phi_1)$, where EPR_2 is not a genuine MES. The average process, as explained in Sec. IID, is responsible for this relatively high value of $E_G^{(2)}$ for the state EPR_2 . Note that for translational symmetric states $E_G^{(2)}$ and $G(2, i_1)$ are equivalent to detect a genuine MES.

However, if we analyze all the $G(2, i_1)$ terms we are able to detect a common characteristic shared only by the genuine MES: for all i_1 we have $G(2, i_1)(\Phi_j, \chi) \geq G(2, i_1)(GHZ_4) = 2/3$. This suggests the following operational definition of a genuine MES:

Definition 1 Let $|\Psi\rangle$ be a pure state describing four qubits. If $G(1) = 1$ and $G(2, i_1)(\Psi) \geq G(2, i_1)(GHZ_4) = 2/3$, $i_1 = 1, 2, 3$, then $|\Psi\rangle$ is a genuine MES.

Besides being practical, Definition 1 has a simple physical interpretation if we remember that $E_G^{(2)}$ and $G(2, i_1)$ are constructed in terms of the linear entropy of any two qubits with the rest of the chain. Noting that the linear entropy is related to the purities of the two-qubit reduced density matrices, the definition above establishes an upper bound for all the two-qubit purities of a MES. In other words, if all the two-qubit purities are below this upper bound the N qubit state can be considered a genuine MES [28]. Furthermore, this upper bound was chosen to be that of the GHZ state, which is undoubtedly a genuine MES. One last remark, since $G(2, i_1)$ is a monotonically decreasing function of the purities an upper bound for the purities implies a lower bound for the value of $G(2, i_1)$ for any genuine MES (cf. Definition 1).

We can easily generalize this definition to N qubits if we express it in terms of all n -qubit purities ($n < N$):

Definition 2 A pure state of N qubits $|\Psi\rangle$ is a genuine MES if

$$\begin{aligned} \text{Tr}(\rho_{j_1}^2) &\leq \text{Tr}(\sigma_1^2) = 1/2, \\ \text{Tr}(\rho_{j_1, j_2}^2) &\leq \text{Tr}(\sigma_{1,2}^2) = 1/2, \\ &\vdots \\ \text{Tr}(\rho_{j_1, j_2, \dots, j_n}^2) &\leq \text{Tr}(\sigma_{1,2, \dots, n}^2) = 1/2, \end{aligned}$$

where

$$\begin{aligned}\rho_{j_1, j_2, \dots, j_n} &= \text{Tr}_{j_1, j_2, \dots, j_n}(|\Psi\rangle\langle\Psi|), \\ \sigma_{1, 2, \dots, n} &= \text{Tr}_{1, 2, \dots, n}(|GHZ_N\rangle\langle GHZ_N|),\end{aligned}$$

and

$$\begin{aligned}1 &\leq j_1 \leq N, \\ 1 &\leq j_1 < j_2 \leq N, \\ &\vdots \\ 1 &\leq j_1 < j_2 < \dots < j_n \leq N.\end{aligned}$$

Note that as we increase the size of the chain we need to calculate more and more purities. Take for instance the state GHZ_3^2 given by Eq. (31). A direct calculation gives $\text{Tr}(\rho_{j_1}^2) = 1/2$ for $1 \leq j_1 \leq 6$, $\text{Tr}(\rho_{3,4}^2) = 1/4$, and $\text{Tr}(\rho_{j_1, j_2}^2) = 1/2$ for all $1 \leq j_1 < j_2 \leq 6$ but $(j_1, j_2) = (3, 4)$. Hence, if we restricted Definition 2 to reduced density matrix of just one and two qubits we would erroneously conclude that GHZ_3^2 is a genuine MES. Extending, however, the definition to all possible reduced density matrices we can detect that GHZ_3^2 is not a genuine MES since $\text{Tr}(\rho_{1,2,3}^2) = 1$, a clear violation of Definition 2.

We end this section calling attention to the fact that Definition 2 are well defined for finite chains only. For infinite chains $N \rightarrow \infty$ and it does not make sense to calculate all $G(2, i_1)$. Finally, the previous definition does not imply that all genuine MES must have $\text{Tr}(\rho_j^2) \leq 1/2$, $\text{Tr}(\rho_{j, j+i_1}^2) \leq 1/2$, \dots , $\text{Tr}(\rho_{j, j+i_1, \dots, j+i_{n-1}}^2) \leq 1/2$. It is only a sufficient condition for a state to be a genuine MES.

B. Infinity Chains

As we have seen in the previous section, for a system with translational symmetry, as the Ising model, the generalized global entanglement is easily evaluated. In addition to this, the Ising model has a quantum phase transition (QPT) where at the critical point the correlation length is infinity. This suggests interesting entanglement properties for the ground state and compels us to study the Ising model ground state entanglement properties. (We should mention that there exist other interesting studies on the relation between entanglement and QPT [17, 18, 29, 30]). In this perspective, here we obtain $G(1)$, which is shown to behave similar to the von Neumann entropy calculated in Ref. [29], and $G(2, i_1)$ for some values of i_1 .

The Ising model with a transverse magnetic field is given by the Hamiltonian

$$H = \lambda \sum_i^N \sigma_i^x \sigma_{i+1}^x + \sum_i^N \sigma_i^z. \quad (37)$$

This model has a symmetry under a global rotation of 180° over the z axes ($\sigma^x \rightarrow -\sigma^x$) which demands that $\langle \sigma^x \rangle = 0$. However as we decrease the magnetic field, increasing λ , this symmetry is spontaneously broken (in the thermodynamic limit) and we can have a ferromagnetic phase with $\langle \sigma^x \rangle \neq 0$. This phase transition occurs at the critical point $\lambda = \lambda_c = 1$ where the gap vanishes and the correlation length goes to infinity. This transition is named quantum phase transition since it takes place at zero temperature and has many of the characteristics of a second order thermodynamic phase transition: phase transitions where the second derivative of the free energy diverges or is not continuous.

It is worth noting that in the thermodynamic limit for $\lambda > 1$ the ground state is two fold degenerated. These two states have opposite magnetization. Here we will use the broken symmetric state for $\lambda > 1$ and not a superposition of the two degenerated states, which is also a ground state but unstable. For a more detailed discussion see Refs. [29, 31].

Now, let us explain how we can evaluate $G(1)$ and $G(2, i_1)$ for the one dimensional Ising model. We need, then, the reduced density matrix of two spins, which is 4×4 matrix and can be written as

$$\rho_{ij} = \text{Tr}_{\overline{ij}}(\rho) = \frac{1}{4} \sum_{\alpha, \beta} p_{ij}^{\alpha\beta} \sigma_i^\alpha \otimes \sigma_j^\beta. \quad (38)$$

The coefficients are given by

$$p_{ij}^{\alpha\beta} = \text{Tr}(\sigma_i^\alpha \sigma_j^\beta \rho_{ij}) = \langle \sigma_i^\alpha \sigma_j^\beta \rangle, \quad (39)$$

and, as usual, $\text{Tr}_{\overline{ij}}$ is the partial trace over all degrees of freedom except the spins at sites i and j , σ_i^α is the Pauli matrix acting on the site i , $\alpha, \beta = 0, x, y, z$ where σ^0 is the identity matrix, and the coefficients $p_{ij}^{\alpha\beta}$ are real.

Eq. (39) shows that all we need are the two-point spin correlation functions which, in principle, are at most 16. This number can be reduced using the symmetries of the Hamiltonian (37). The translational symmetry implies that ρ_{ij} depends only on the distance $|i - j| = n$ between the spins so that we have $p_{ij}^{\alpha\beta} = p_n^{\alpha\beta}$ and $p_n^{\alpha\beta} = p_n^{\beta\alpha}$. Besides this we also have $\rho_n^* = \rho_n$ since the Hamiltonian is real. All these symmetries imply that the only non-zero correlations functions are: $p_n^{\alpha\alpha}$, $p^{0x} = p^{x0} = p^x$, $p^{0z} = p^{z0} = p^z$, and $p_n^{xz} = p_n^{zx}$.

First, let us show the diagonal correlation functions and the magnetizations, which were already calculated in Ref. [32]. For periodic boundary conditions and an infinite chain we have:

$$\langle \sigma_i^x \sigma_{i+n}^x \rangle = \begin{vmatrix} g(-1) & g(-2) & \dots & g(-n) \\ g(0) & g(-1) & \dots & g(-n+1) \\ \vdots & \vdots & \ddots & \vdots \\ g(n-2) & g(n-3) & \dots & g(-1) \end{vmatrix}, \quad (40)$$

$$\langle \sigma_i^y \sigma_{i+n}^y \rangle = \begin{vmatrix} g(1) & g(0) & \cdots & g(-n+2) \\ g(2) & g(1) & \cdots & g(-n+3) \\ \vdots & \vdots & \ddots & \vdots \\ g(n) & g(n-1) & \cdots & g(1) \end{vmatrix}, \quad (41)$$

$$\langle \sigma_i^z \sigma_{i+n}^z \rangle = \langle \sigma^z \rangle^2 - g(n)g(-n), \quad (42)$$

$$\langle \sigma^z \rangle = g(0), \quad (43)$$

and

$$\langle \sigma^x \rangle = \begin{cases} 0, & \lambda \leq 1 \\ (1 - \lambda^{-2})^{1/8}, & \lambda > 1 \end{cases}, \quad (44)$$

with

$$g(n) = l(n) + \lambda l(n+1) \quad (45)$$

and

$$l(n) = \frac{1}{\pi} \int_0^\pi dk \frac{\cos(kn)}{1 + \lambda^2 + 2\lambda \cos(k)}. \quad (46)$$

We are now left with the evaluation of $p_n^{xz} = p_n^{zx}$. This calculation was made in Ref. [33] where the authors obtained the off-diagonal, time and temperature dependent, spin correlation functions. In the paramagnetic phase ($\lambda \leq 1$) the fundamental state has the same symmetries of the Hamiltonian which leads to $p_n^{xz} = 0$. For the ferromagnetic phase ($\lambda > 1$) an explicit evaluation leaves us with an expression in terms of intricate complex integrals which are not straightforward to compute. For this reason we will use bounds for this off-diagonal correlation function.

We can obtain an upper and lower bound for this correlation function using the Cauchy-Schwarz inequality [10]. Consider generic states $|a\rangle$ and $|b\rangle$ and generic observables A and B . The Cauchy-Schwarz inequality states that $|\langle a|b\rangle| \leq \sqrt{\langle a|a\rangle\langle b|b\rangle}$. For $|a\rangle = A|\psi\rangle$ and $|b\rangle = B|\psi\rangle$ the Cauchy-Schwarz inequality reads $|\langle AB\rangle| \leq \sqrt{|\langle A^2\rangle\langle B^2\rangle|}$. Here $|\psi\rangle$ is any normalized state (the Ising model ground state for instance) and the brackets denote expectation values of the operators for a system described by $|\psi\rangle$.

For the infinite Ising model it can be shown [32] that $\langle \sigma_x^2 \rangle = \langle \sigma_x \rangle^2$ and that $\langle \sigma_z^2 \rangle = \langle \sigma_z \rangle^2$. Therefore, if $A = \sigma^x$ and $B = \sigma^z$ we have $|\langle \sigma^x \sigma^z \rangle| \leq |\langle \sigma^x \rangle \langle \sigma^z \rangle|$. This is an upper bound for the absolute value of the two-point correlation function $\langle \sigma^x \sigma^z \rangle$. Note that this bound does not depend on the distance between the spins and it is the true value of $|\langle \sigma^x \sigma^z \rangle|$ in the limit $n \rightarrow \infty$ [32]. Since in the calculations of $E_G^{(1)} = G(1)$ and $G(2, i_1)$ we only need squares of correlation functions (c.f. Eqs. (47) and

(48)) we can work with the following lower and upper bounds for $\langle \sigma^x \sigma^z \rangle^2$,

$$0 \leq \langle \sigma^x \sigma^z \rangle^2 \leq \langle \sigma^x \rangle^2 \langle \sigma^z \rangle^2.$$

Another approach to find bounds is by imposing the positivity of the eigenvalues of the reduced density operator ρ_{ij} . For the Ising model these bounds result to be much tighter than the previous ones obtained via the Cauchy-Schwarz inequality, as we can see in Fig. 7, and depend on n . For these reasons, we employ these bounds for p_n^{xz} in the following calculations. In Ref. [10] some of the results here discussed were presented using the bounds obtained from the Cauchy-Schwarz inequality.

It is worth mentioning that since $G(1)$ and $G(2, i_1)$ are decreasing functions of the square of the correlation functions, a lower (upper) bound for the latter implies a upper (lower) bound for the former.

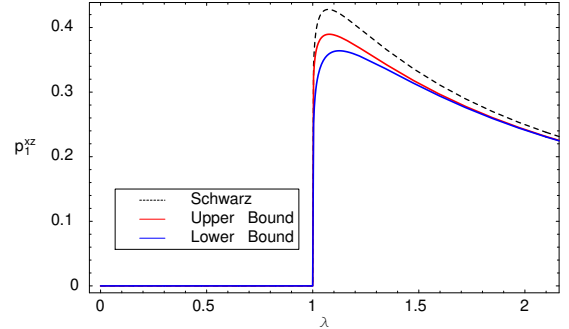


Figure 7: (Color online) Bounds for p_n^{xz} obtained by the Cauchy-Schwarz inequality (dashed) and by imposing positivity of the eigenvalues of the reduced density operator ρ_{ij} (solid).

Now that we have all the correlation functions we need we proceed in the calculations of $G(1)$ and $G(2, i_1)$. Remembering that for the Ising model $p^y = 0$ Eq. (20) can be written as

$$G(1) = 1 - (p^x)^2 - (p^z)^2. \quad (47)$$

As we have already shown $G(1)$ is the mean linear entropy of one spin which, due to translational symmetry, is equal to the linear entropy of any spin. A similar related analysis was done by Osborne and Nielsen [29]. Instead of the linear entropy they have employed the von Neumann entropy between one spin and the rest of the chain. As well as $G(1)$ (See Fig. 9), the von Neumann entropy is maximal at the critical point [29]. At that time Osborne and Nielsen did not give great importance to this result since they suspected that the von Neumann entropy of one spin with the rest of the chain does not measure genuine MES. However, for a translational symmetric state it is a fairly good indication of genuine ME as we have shown in previous sections. (We have explicitly studied linear entropy but the same results apply to the von Neumann entropy. We have adopted the former mainly

because of its simplicity and relation to the Meyer and Wallach global entanglement [11]).

Analyzing Eq. (47) we can understand why $G(1)$ is maximal at the critical point ($\lambda = 1$). As we explain in what follows, it is $\langle \sigma^x \rangle$ the main responsible for this behavior of $G(1)$. For $\lambda \leq 1$ $\langle \sigma^x \rangle = 0$. After the critical point, however, $\langle \sigma^x \rangle \neq 0$. Moreover, Eq. (44) tells us that for $\lambda > 1$ $\langle \sigma^x \rangle$ is a monotonic increasing function of λ and that $\langle \sigma^x \rangle \rightarrow 1$ as $\lambda \rightarrow \infty$. Therefore, since $\langle \sigma^z \rangle$ is negligible for large values of λ and $\langle \sigma^x \rangle \approx 1$ (See Fig. 8) we must have $G(1)$ approaching zero after the critical point.

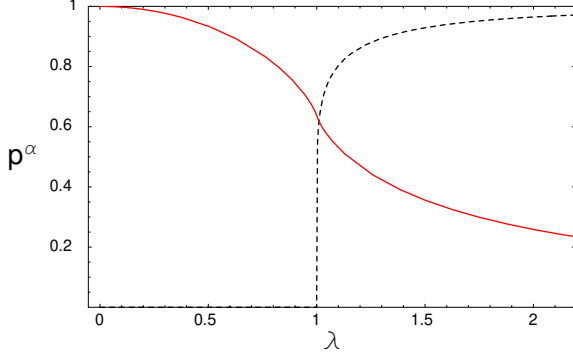


Figure 8: (Color online) Magnetizations $p^z = \langle \sigma^x \rangle$ (black/dashed line) and $p^z = \langle \sigma^z \rangle$ (red/solid line) as a function of λ .

We now move to the study of $G(2, i_1)$. Using the Ising model symmetries Eq. (24) reads,

$$G(2, n) = 1 - \frac{1}{3} [2(p^x)^2 + 2(p^z)^2 + 2(p^{xz})^2 + (p_n^{xx})^2 + (p_n^{yy})^2 + (p_n^{zz})^2]. \quad (48)$$

With the definition above we can evaluate $G(2, n)$ for any value of n . In Fig. 9 we have plotted $G(1)$ and the bounds for $G(2, 1)$. We can see that both $G(1)$ and $G(2, 1)$ are maximum at the critical point $\lambda = 1$. Note that the bounds are very tight and can barely be distinguished just in a small region near $\lambda = 1$. Furthermore $G(2, 1)$ is always smaller than $G(1)$ contrary to what was obtained using the Cauchy-Schwarz bounds in Ref. [10]. As well as in the case of $G(1)$ we can see that the reason for $G(2, 1)$ being maximal at the critical point is due to the behavior of $\langle \sigma^x \rangle$ since it is the only function in Eq. (48) that does not change smoothly as we cross the critical point (see Fig. 10 for the other correlation functions).

We have also plotted $G(2, n)$ for $n = 1, 7$ and 15 (Fig. 11). We can observe that all of them are maximum at the critical point and increase as a function of n (In Fig. 11 we have plotted only the upper bounds since the lower bounds produce very similar curves). We also note that $G(2, 7)$ is very near $G(2, 15)$ showing that $G(2, n)$ rapidly saturates to a fixed value. At the critical point we have $\lim_{n \rightarrow \infty} G(2, n) = 0.675$. This behavior for $G(2, n)$ points in the direction of the existence of multipartite

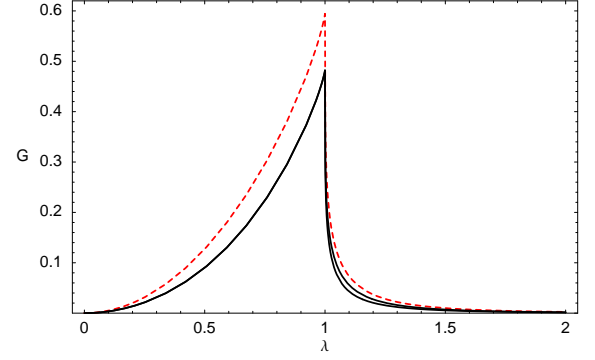


Figure 9: (Color online) $G(1)$ (red/dashed line) and the bounds for $G(2,1)$ (black/solid line). Note that they are maximum at the critical point.

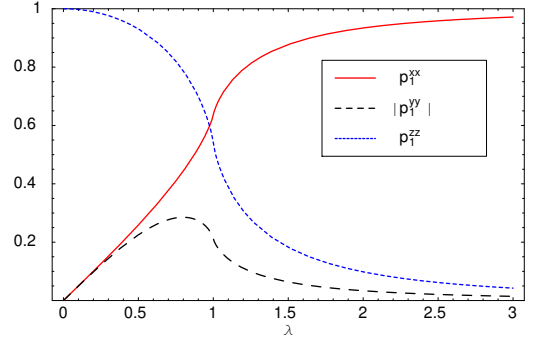


Figure 10: (Color online) Two point correlation functions: p_1^{xx} (red/solid), $-p_1^{yy}$ (black/long-dashed), and p_1^{zz} (blue/short-dashed).

entanglement at the critical point since any two spins are entangled with the rest of the chain and this entanglement increases with the distance between them. It is also interesting to confront this result with the fact that two spins that are separated by two or more sites are not entangled since their concurrences are zero [30].

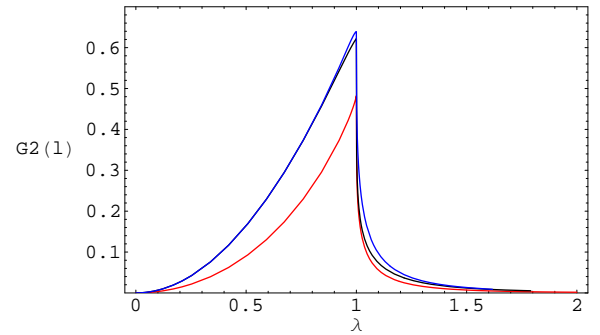


Figure 11: (Color online) $G(2, n)$ for $n = 1, 7$ and 15 . From bottom to top $n = 1, 7$ and 15

The behavior of the concurrence ($C(n)$) can also be understood if we note that it can be expressed in terms

of the one and two point correlation functions. While for the non-symmetric (ferromagnetic) state the analytical expression for the concurrence is cumbersome for the symmetric one it is very simple. Fortunately, for the Ising model it was shown that the concurrence does not change upon symmetry break [19, 20] and we get

$$C(n) = \frac{1}{2} (-1 - p_n^{yy} + p_n^{xx} + p_n^{zz}). \quad (49)$$

From this expression we can see that the concurrence (Fig. 12) does not depend on either the off-diagonal correlation function (p_n^{xz}) or on the one point correlation function (magnetizations). This helps us to understand why the concurrence is not maximum at the critical point.

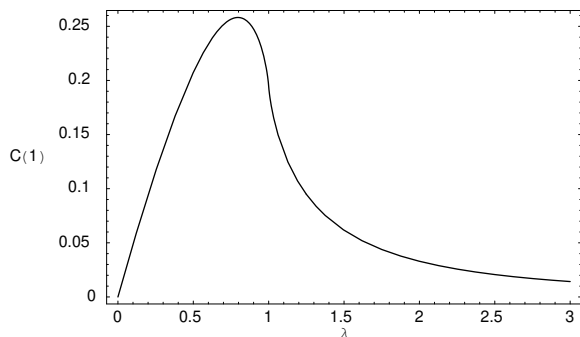


Figure 12: Concurrence for nearest neighbors.

IV. CONCLUSION

In this article we have formalized an operational multipartite entanglement measure introduced in Ref. [10]

which is a direct generalization of global entanglement [11]. We have called such a measure *generalized global entanglement* ($E_G^{(n)}$), being the first class ($n = 1$) exactly the Meyer and Wallach global entanglement [11].

We have shown that for some systems composed of many subsystems, the original global entanglement is not able to properly classify and identify multipartite entanglement in a unequivocally way, whereas higher classes of $E_G^{(n)}$ are. We have calculated $E_G^{(n)}$ for a variety of multipartite entangled qubit states. Specifically, we have shown that the genuine multipartite entangled states (MES) presented in Refs. [23, 24] are all distinguished by $E_G^{(2)}$ and $G(2, i_1)$, whereas Meyer and Wallach global entanglement [11] fails to discriminate among them ($E_G^{(1)} = 1$ for all of them). We have also presented an operational definition of a genuine MES inspired by a common characteristic for the values of $G(2, i_1)$ obtained for some paradigmatic genuine MES [23, 24].

Furthermore, we have shown that $E_G^{(2)}$ and $G(2, i_1)$ are all maximal at the quantum critical point of the Ising model in a transverse magnetic field. It is an interesting result since the maximality of $G(2, i_1)$ suggests that at the quantum phase transition ($\lambda = 1$) we have a genuine MES.

Acknowledgments

GR and TRO acknowledge financial support from Fundação de Amparo à Pesquisa do Estado de São Paulo (FAPESP) and MCO acknowledges support from FAPESP and FAEPEX-UNICAMP.

-
- [1] E. Schrödinger, Proc. Camb. Phil. Soc. **31**, 555 (1935).
 - [2] A. Einstein, B. Podolsky, and N. Rosen, Phys. Rev. **47**, 777 (1935).
 - [3] J. S. Bell, Physics **1**, 195 (1964).
 - [4] M. A. Nielsen and I. L. Chuang, Quantum Computation and Quantum Information (Cambridge University Press, Cambridge, 2000).
 - [5] W. K. Wootters, Phys. Rev. Lett. **80**, 2245 (1998).
 - [6] S. L. Braunstein and P. van Loock, Rev. Mod. Phys. **77**, 513 (2005).
 - [7] Richer classifications with more parameters can be pursued. For instance, we can have a multipartite state where four subsystems are entangled, another five are entangled, and the remaining subsystems are separable. We would need now two parameters to classify this state.
 - [8] W. Dür, G. Vidal, and J. I. Cirac, Phys. Rev. A **62**, 062314 (2000).
 - [9] F. Verstraete, J. Dehaene, B. De Moor, and H. Verschelde, Phys. Rev. A **65**, 052112 (2002).
 - [10] T. R. Oliveira, G. Rigolin, and M. C. Oliveira, Phys. Rev. A **73**, 010305(R) (2006).
 - [11] D. A. Meyer and N. R. Wallach, J. Math. Phys. **43**, 4273 (2002).
 - [12] H. Barnum, E. Knill, G. Ortiz, R. Somma, and L. Viola, Phys. Rev. Lett. **92**, 107902 (2004).
 - [13] R. Somma, G. Ortiz, H. Barnum, E. Knill, and L. Viola, Phys. Rev. A **70**, 042311 (2004).
 - [14] G. K. Brennen, Quantum Inf. Comp. **3**, 619 (2003).
 - [15] A. Lakshminarayan and V. Subrahmanyam, Phys. Rev. A **71**, 062334 (2005).
 - [16] A. J. Scott, Phys. Rev. A **69**, 052330 (2004).
 - [17] J. I. Latorre, E. Rico, and G. Vidal, Quantum Inf. Comp. **4**, 48 (2004) and references therein.
 - [18] G. Vidal, J. I. Latorre, E. Rico, and A. Kitaev, Phys.

- Rev. Lett. **90**, 227902 (2003).
- [19] O. F. Syljuåsen, Phys. Rev. A **68**, 060301(R) (2003).
- [20] O. F. Syljuåsen, eprint quant-ph/0312101.
- [21] D. M. Greenberger, M. A. Horne, A. Shimony, and A. Zeilinger, Am. J. Phys. **58**, 1131 (1990).
- [22] G. Rigolin, Phys. Rev. A **71**, 032303 (2005).
- [23] A. Osterloh and J. Siewert, Phys. Rev. A **72**, 012337 (2005).
- [24] Y. Yeo and W. K. Chua, Phys. Rev. Lett. **96**, 060502 (2006).
- [25] V. Coffman, J. Kundu, and W. K. Wootters, Phys. Rev. A **61**, 052306 (2000).
- [26] C. P. Yang and G. C. Guo, Chin. Phys. Lett. **17**, 162 (2000).
- [27] G. Vidal and R. F. Werner, Phys. Rev. A **65**, 032314 (2002).
- [28] Another way of interpreting Definition 1 is to consider it as a sufficient condition for a state to be a genuine MES.
- [29] T. J. Osborne and M. A. Nielsen, Phys. Rev. A **66**, 032110 (2002).
- [30] A. Osterloh, L. Amico, G. Falci and R. Fazio, Nature **416**, 608 (2002).
- [31] S. Sachdev, *Quantum Phase Transitions* (Cambridge University Press, Cambridge, 1999).
- [32] P. Pfeuty, Ann. Physics (New York) **57**, 79 (1970).
- [33] J. D. Johnson and B. M. McCoy, Phys. Rev. A **4**, 2314 (1971).